A Report on the Snow Conditions of the North Slope and Brooks Range of Alaska during the Winter of 2018

Geophysical Institute-UAF Occasional Report-82018

August 20, 2018

Funding for this report was supplied by NASA, the National Science Foundation and the Geophysical Institute, with logistical support from the U.S. Fish and Wildlife Service.

A Report on the Snow Conditions of the North Slope and Brooks Range of Alaska during the Winter of 2018

Dr. Matthew Sturm, Geophysical Institute, U. of Alaska Fairbanks (msturm1@alaska.edu)
Mr. Charles L. Parr, Geophysical Institute, U. of Alaska Fairbanks (cparr4@alaska.edu)
Dr. Stine Højlund Pedersen, Dept. of Biological Sciences, U. of Alaska Anchorage (spedersen3@alaska.edu)
Dr. Chris Arp, University of Alaska Fairbanks, WERC (cdarp@alaska.edu)
Mr. Frank Urban, USGS Denver (furban@usgs.gov)
Dr. Jeff Welker, Dept. of Biological Sciences, University of Alaska Anchorage (jmwelker@alaska.edu)
Dr. Mark Serreze, National Snow and Ice Data Center (serreze@nsidc.org)

Communications regarding this report should be directed to Dr. Matthew Sturm

Introduction

The Brooks Range and North Slope stretch from the Canadian border to the west coast of Arctic Alaska, encompassing an area of over 250,000 km^2. This region is blanketed with snow from late-September through June, more than 9 months each year. This snow cover is the source of much of the run-off from the area, plays a key role in the thermal state of the underlying permafrost, and determines icing conditions on rivers and lakes. It is also a critical element in the habitat of the animals and birds of the region, affecting how they forage, den, travel and migrate. A fundamental character of this snow cover is that it is heterogeneous; deep drifts often exist adjacent to areas where the tundra is virtually bare of snow all winter.

Despite the widespread and obvious importance of snow, relatively few snow measurements are available from the region. The limited data reflects that the region is sparsely inhabited and mostly roadless. Much of the data that is available come from autonomous weather stations, chiefly RAWS (Remote Automatic Weather Stations: https://raws.dri.edu/akF.html) installations operated by the Desert Research Institute for the National Park Service (NPS), SNOTEL sites operated by the National Resource Conservation Service (NRCS: NRCS website), and a series of stations installed by the USGS primarily for studies related to permafrost and climate change (GTN-P; https://pubs.usgs.gov/ds/812/introduction.html). Just two manned NOAA Weather Service (NWS) stations are found in the region (Barrow (*Utqiagvik*) and Kotzebue), so with these two few exceptions, normal snow data are collected by electronic instruments. Over much of the region and most of the time, the actual snow conditions are not observed by humans. One consequence of this is that there is no easy way to ascertain whether the instrument measurements are reporting good data. Moreover, virtually all of the values of snow depth and snow water equivalent (SWE) collected autonomously from these networks are "spot" values, typically reflecting conditions from an area less than 1 m^2 in size adjacent to the tower. There is no easy way to know if just a few meters away, the conditions are quite different.

More specifically, the RAWS and GTN-P sites report snow depth using sonic sounders that sample about 0.25-m^2, not a very big sample. The NRCS report depth in the same way, but also record snow water equivalent (SWE) using totaling precipitation gauges. Crtical snow properties like hardness, layering, density, and suitability for over-snow travel, all of which contribute to the overall impact of the snow in the region on animals, plants, and human activity, are not measured anywhere in the region by humans, nor have they been measured in the past.

Consequently, for this vast region, we have almost no baseline or historical record against which we can examine current conditions and detect trends due to a changing climate.

With that knowledge gap in mind, an unusual situation occurred in late-winter and spring of 2018: four grant-funded research groups made extensive snow measurements across the region in March, April and early-May, a period during which there was little additional snowfall. When these data were combined, it presented an opportunity to examine the snow cover over a wide area independent of the existing instrument network. Here we present these data (which include over 39,000 individual depth measurements), explore what they tell us about the regional snow cover, and compare the data to the values recorded by the autonomous instruments. As it turns out, the winter of 2017-2018 produced one of the deepest and long-lasting snow covers in the past 30 years, making the result particularly interesting.

Field Area

Figure 1 shows the region over which the snow measurements were made. Much of the field work originated from Toolik Lake Field Station, hence the high density of measurements near there. The measurements were made between March 4th and May 2rd, 2018, during which time there was little new snowfall and not much wind. We think it is therefore reasonable to view the data set as simultaneous; i.e., essentially as if it were taken at single time. We refer to this as the late-winter snow pack of 2018. Unfortunately, no measurements were made in the far western end of the study area, so snow conditions there remain an unknown.

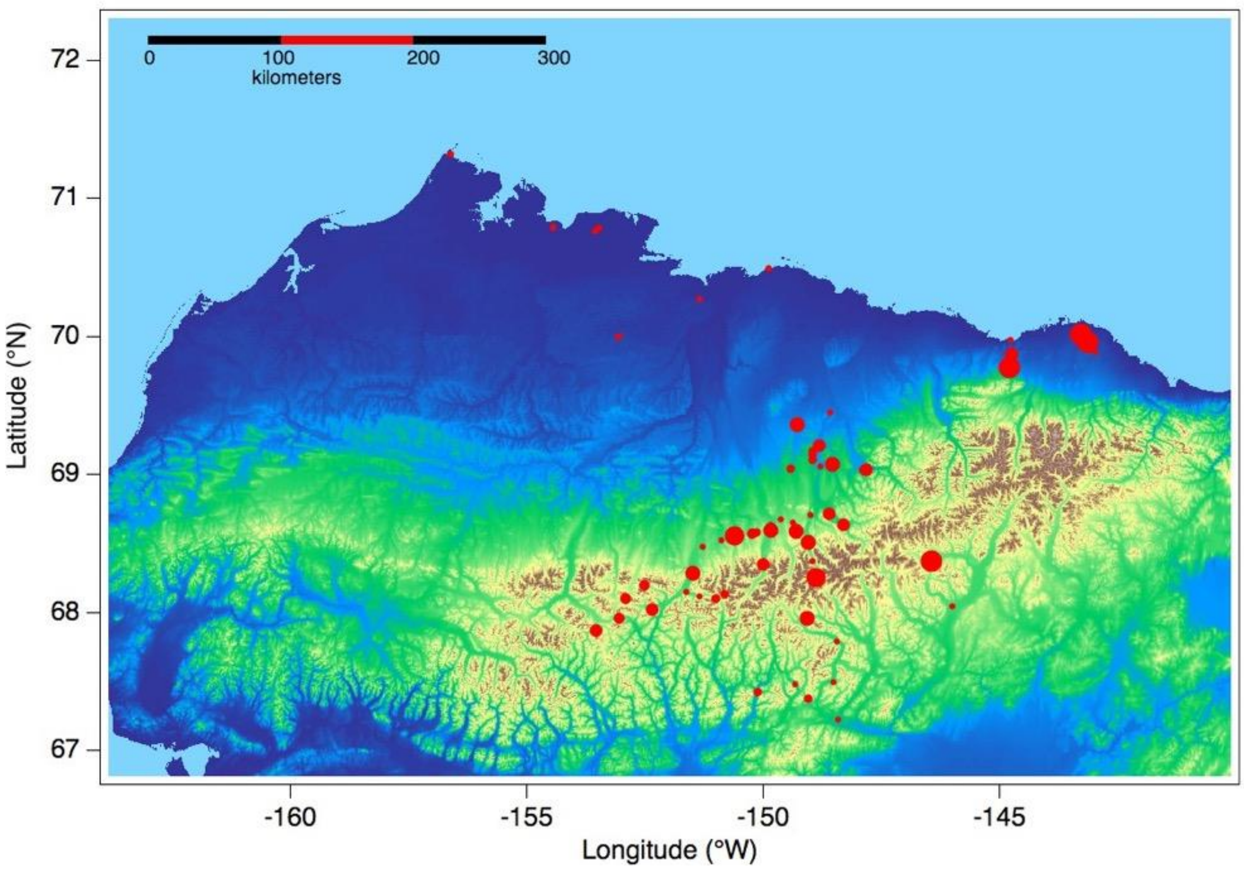

Figure 1: The study area. Measurement locations are shown by the red circles, with the relative number of measurements (mostly depth) suggested by the circle size (ranging from 10 to several thousand values). The results come from four research groups (see author list).

The data shown in Figure 1 have been derived from four separate research groups (see author list) and in many cases consisted of depth measurements only. However, a more comprehensive set of measurements were made during an 800-km snowmobile traverse from Toolik Lake to the west and return (stations shown in Fig. 2). At stations along this traverse measurements included depth probing along transect lines, density measurements, stratigraphic and texture measurements, coring for snow water equivalent, and wind drift mapping. These more comprehensive data are used below to explore the snow density, hardness and other attributes.

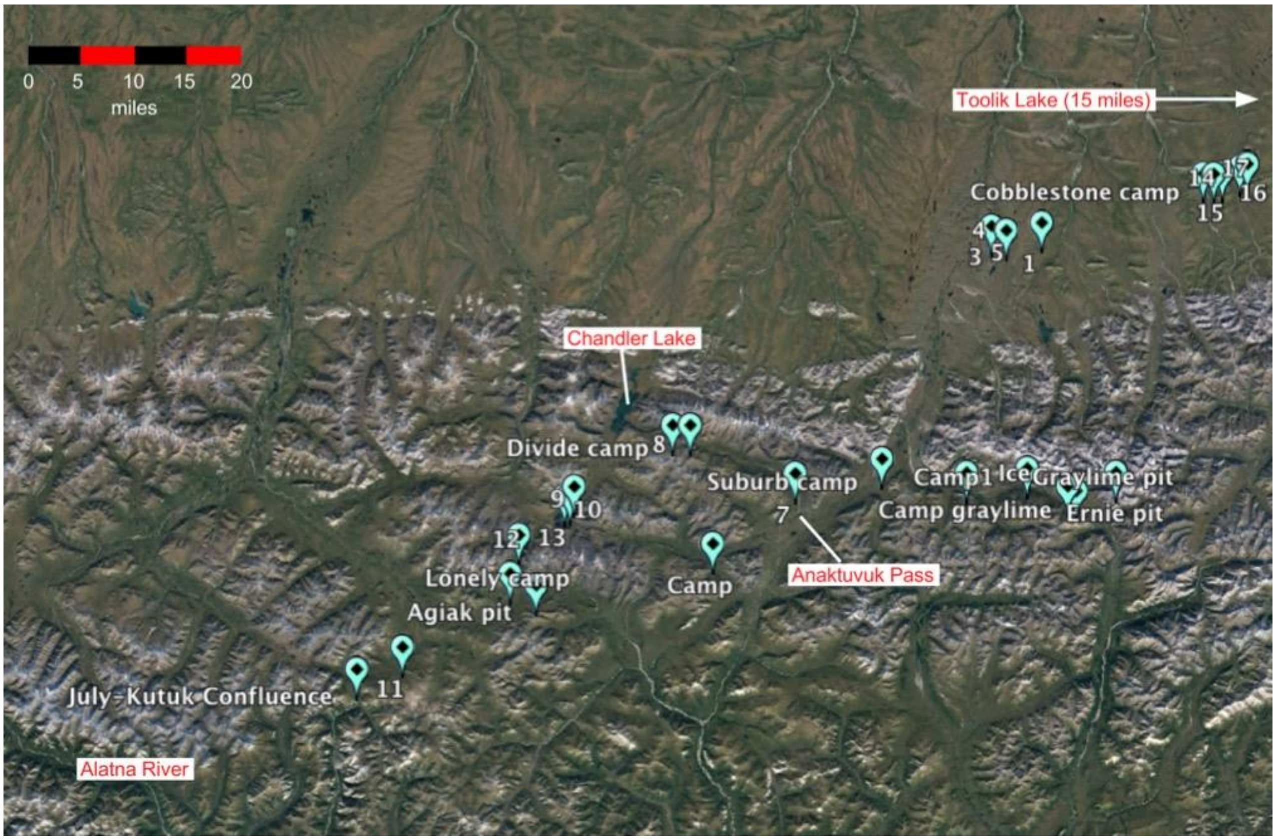

Figure 2: Location of more detailed snow measurements.

Methods: “Neutral” areas were sought when selecting measurement stations, *i.e.*, areas where neither wind scour nor deposition had occurred. These areas are typically flat, have vegetation characteristic of the surrounding locality, and show little sign of wind action. Faced with the huge and extremely diverse snow landscape that makes up the study area (Figs. 1, 2 and 3), we believe picking such stations is the only practical way to capture the large-scale trends in the snow cover. The measurement locations shown in Figure 2 were generally about a day’s snowmobile travel apart (20 to 50 km) and were quasi-random in their location in that we had not selected the locations in advance. They were selected in the field by noting that we had traversed far enough, then looking around for flat, non-wind affected areas. The spacing of the measurements in Figure 1 is greater and more random, reflecting the various research objectives of the four groups.

Figure 3: The view to the NE at the headwaters of the N. Fork, Koyukuk River showing deep snow among the willows, scoured snow in the middle ground on ridges, and drifted snow in gullies. Choosing a neutral area here was challenging, but ultimately possible (e.g."Ernie Pit" on Figure 2).

Depth measurements were generally made using a GPS-enabled automatic snow depth probe (Magnaprobe, U.S. Patent 5,864,059), with depth and location measured along one or several legs radiating from a central location. The legs varied from about 100 to over 500-m in length. Allowing for the potential to over-probe (the probe penetrating soft ground beneath the snow), we estimate depth values were accurate to better than +5 cm. Typically at least 100 depths were collected along a line at 1.5 to 3.0 m spacing.

SWE measurements were made using a Federal Sampler. This is the standard coring tool used by the NRCS throughout its western U.S. network. The aluminum cylindrical sampler has a cross-sectional area of 11.46 cm^2 and a serrated steel cutter edge. The accuracy of SWE measurements taken this way has been investigated and varies widely with snow quality and operator skill. With care, bulk snow density and SWE values accurate to ±15% can be achieved, though we have found the device has a low bias. Typically, we collected 10 cores at each location (see also *Snow Pits*), two near the snow pit, and an additional 8 cores on a line running north from the pit, the cores done in pairs with each pair about 20 m north of the previous core. Core samples were bagged and weighed immediately after collection using a digital balance accurate to 0.01 g.

Snow pit measurements were done using the following protocol: at each location (Fig. 4) a snow trench was dug that was about 2.5 meters wide. From the wall of the trench we recorded the snow layering, the layer density (in duplicate or triplicate), the hardness, grain characteristics, and the thickness of each layer. Two Federal cores bracketing the pit were collected so that they that could be compared directly to the integrated bulk density computed from layer densities. Two orthogonal snow depth probe lines radiated from the pit outward. Photographs of the pit and the surrounding landscape (4 cardinal directions) were general taken for reference.

Snow Isotopes measurements were made on snow samples collected from the snow pits. We measured $\delta^{18}O$, $\delta^{2}H$ and *d-excess* values as surrogates for moisture sources in order to deduce the storm tracks that deposited the snow. Samples were taken from the top and the bottom of the pits, and we primarily compared results from samples taken north of the Brooks Range with those taken from the south. A long-term record of isotope geochemistry in Alaska and across the US provides the basis for some of our interpretation and the use of this approach.

Winter Wind Directions were inferred from surrounding drift features. We created sketch maps in the field of general wind/snow transport directions. These were inferred from a) cornices, b) scour zones, c) crag and tail feathers, and d) wind waves, dunes and barchans. In making these maps, we focused on the larger features that had been created over much of the winter, rather than in the most recent wind/snow events.

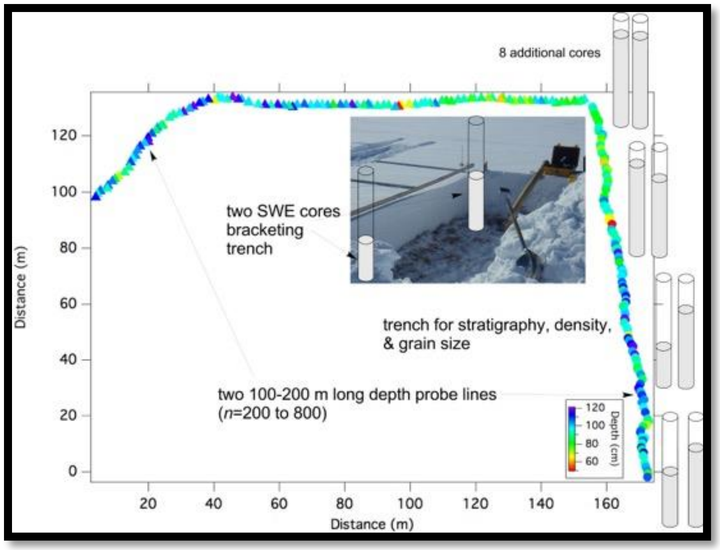

Figure 4: A general layout of snow pit, core locations, and depth probe lines.

Aerial Snow Mapping: We used structure from motion (SfM) mapping techniques to produce snow depth maps over three areas, each about 4 by 16 km in extent. These maps have a ground resolution of 1-m, and can resolve snow depth to ±0.1m. The technique we used is highly accurate, and is described in detail in a publication by M. Nolan, C. Larsen and M. Sturm (Nolan, M., Larsen, C. F., & Sturm, M. (2015). *Mapping snow-depth from manned-aircraft on landscape scales at centimeter resolution using Structure-from-Motion photogrammetry*. ***Cryosphere Discussions***, ***9***(1)). The areas mapped consisted of (1) a N-S swath near Happy Valley, Alaska, (2) a swath from Toolik Lake Field Station east, and (3) a swath from the Sadlerochit Mountains north to the Arctic Coast at Camden Bay.

Results

The mean snow depth based on the average value at each station (Table I; note that *n* is highly variable by station) was 53.5 cm (*n*=39,972), and the mean value weighted by the number of observations (*n*) was just slightly lower (53.4 cm). The mean standard deviation was 15.4 cm. Depths near the coast were consistently lower than those taken in the Brooks Range (Fig. 5) (both north and south of the crest), as would be expected from prior work, but the full spread in values was not large when considering the range that can be found in seasonal snow covers worldwide. A few of the stations measured and reported in Table I were scoured or drifted. It was these stations that produced the extreme values in the data set (10 and 126 cm) and show up as purple or red markers in Figure 5; they are probably best ignored. A histogram of all depths (Fig. 6) can be fit reasonably well with a log-normal distribution, which has been noted for snow covers in other regions. In part, this fit reflects the fact that zero snow depth is usually rare, but deep drifts are not.

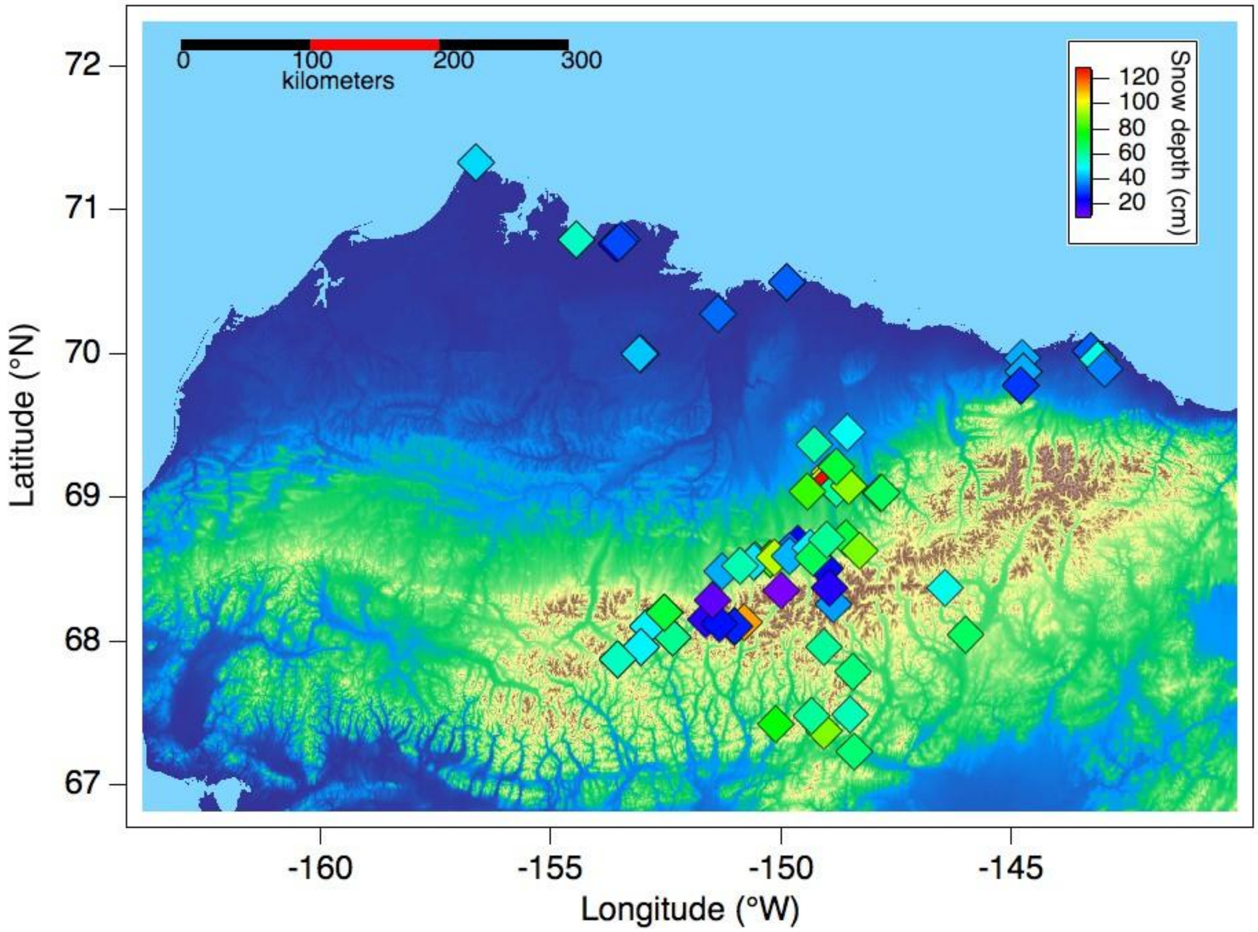

Figure 5: Mean snow depth values at all stations listed in Table I.

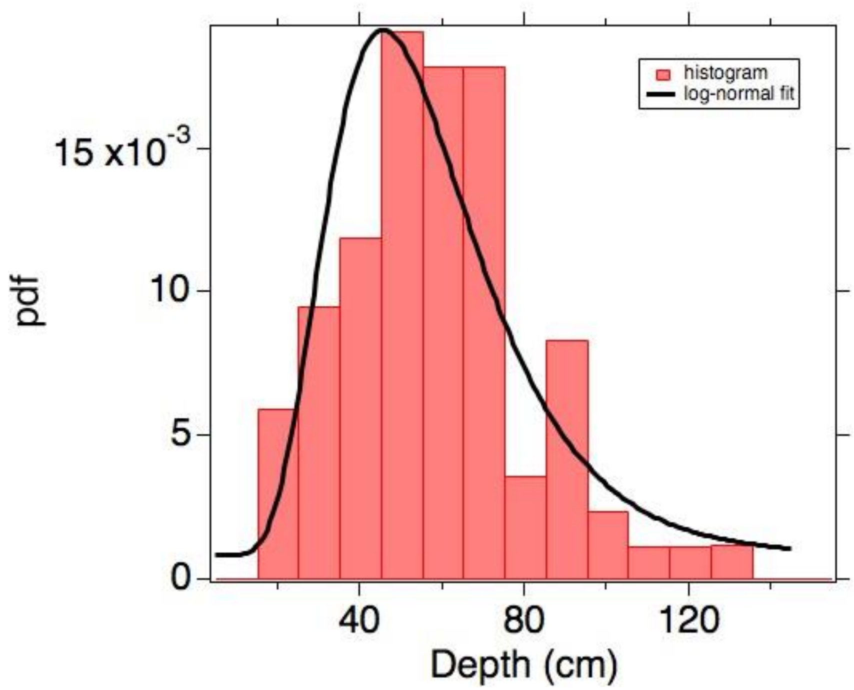

Figure 6: Probability distribution for all snow depth data shown in Table I. The mean value is 53.5 cm (n=39,972).

Table I: Average Snow Depths and Standard Deviations from All Stations

Site	Date	Observer	Location	Latitude	Longitude	num_obs	Ave_depth	Std_dev_depth	Landscape
1	4/14/18	Urban	Camden Bay	69.9718	-144.7707	875	40.2	14.4	
2	4/14/18	Urban	Camden & Mars	69.8693	-144.7323	406	60.2	24.2	
3	4/14/18	Urban	mden & Marsh, l	69.8693	-144.7323	281	56.1	19.8	
4	4/14/18	Urban	Camden & Mars	69.8693	-144.7323	353	40.17	10.4	
5	4/14/18	Urban	larsh Creek, Gec	69.7775	-144.7933	207	25.37	7.82	
6	4/14/18	Urban	h Creek, USGS	69.7775	-144.7933	874	29.15	7.72	
7	4/15/18	Urban	Kaktovik, Geo2	70.0158	-143.2795	854	42.01	15.96	
8	4/15/18	Urban	Kaktovik, Geo1	70.0158	-143.2795	890	32.87	13.48	
9	4/15/18	Urban	(aktovik & Nigua	69.9622	-143.1314	830	46.55	14.3	
10	4/15/18	Urban	(aktovik & Nigua	69.9622	-143.1314	364	51.68	16.41	
11	4/15/18	Urban	Niguanak	69.8893	-142.9842	837	36.17	16.4	
averages:						**6771**	**41.86**	**14.63**	
12	4/30/18	Sturm	alley north end (I	69.1706	-148.9497	193	101.85	38.44	
13	4/30/18	Sturm	/alley cross wate	69.1228	-148.9449	1057	54.3	29.21	
14	5/1/18	Sturm	py Valley filled c	69.1428	-148.9520	271	95.137	32.27	
15	5/1/18	Sturm	/alley crescent l	69.1052	-148.9466	160	126.44	45.77	
						1681	**94.43**	**36.42**	
16	4/28/18	Sturm	Imnavait Grid	68.6130	-149.3128	**3979**	**76.2**	**23.7**	
17	4/15/18	Arp	Ikp-001	70.7900	-154.4510	55	30	1	lake
18	4/15/18	Arp	Ikp-met	70.7940	-154.4350	51	55	8	tundra
19	4/14/18	Arp	Ini-001	69.9960	-153.0710	48	28	3	lake
20	4/14/18	Arp	Ini-002	70.0000	-153.0370	47	10	2	lake
21	4/14/18	Arp	Ini-met	69.9990	-153.0580	45	43	5	tundra
22	4/13/18	Arp	L9819	70.2700	-151.3550	52	34	3	lake
23	4/10/18	Arp	Tes-001	70.7660	-153.5630	50	22	8	lake
24	4/10/18	Arp	Tes-002	70.7890	-153.4700	51	30	5	lake
25	4/10/18	Arp	Tes-met	70.7700	-153.5230	46	31	10	tundra
26	3/27/18	Arp	Too-001	68.6750	-149.6270	47	24	6	lake
27	3/27/18	Arp	Too-002	68.6320	-149.8320	45	34	1	lake
						142	**43**	**7**	
28	5/3/18	Sturm	Oliktok by Gauge	70.4955	-149.8831	555	51.54	13.59	(not including DFIR drift)
29	5/3/18	Sturm	iktok south of roa	70.4947	-149.8814	605	33.32	10.99	
						1160	**42.43**	**12.29**	
30	5/2/18	Sturm	aġvik (Barrow) A	71.3220	-156.6153	**1239**	**45.18**	**11.6**	ot including DFIR drift depths (>80 cm
31	3/6/18	Sturm	uk Divide, Line 1	68.5600	-150.5500	167	49.361	8.799	
32	3/6/18	Sturm	uk Divide, Line 2	68.5600	-150.5500	153	55.56	10.288	
						320	**52.4605**	**9.5435**	
33	3/9/18	Sturm	Ernie Pass, Line1	68.1000	-150.9967	101	84.37	18.08	
34	3/9/18	Sturm	Ernie Pass, Line2	68.1000	-150.9967	140	67.81	30.82	
						241	**76.09**	**24.45**	
35	3/10/18	Sturm	lime Headwall, L	68.1300	-150.8133	nd	nd	nd	
36	3/10/18	Sturm	lime Headwall, L	68.1300	-150.8133	98	110.69	39.89	
						98	**110.69**	**39.89**	
37	3/12/18	Sturm	Ekokpuk, Line 1	68.0217	-152.3517	276	68.022	17.64	
38	3/12/18	Sturm	Ekokpuk, Line 2	68.0217	-152.3517	399	60.34	9.78	
						675	**64.181**	**13.71**	
39	3/13/18	Sturm	hiloyak Lake, Lin	68.1017	-152.9000	223	46.76	11.38	
40	3/13/18	Sturm	hiloyak Lake, Lin	68.1017	-152.9000	218	47.676	5.0265	
						441	**47.218**	**8.20325**	
41	3/14/18	Sturm	Agiak, Line 1	67.9600	-153.0367	232	64.97	19.89	
42	3/14/18	Sturm	Agiak, Line 2	67.9600	-153.0367	252	47.745	9.23	
						484	**56.3575**	**14.56**	
43	3/15/18	Sturm	Creek Divide, Li	67.8683	-153.5400	282	55.293	5.76	
44	3/15/18	Sturm	Creek Divide, Li	67.8683	-153.5400	370	55.32	6.52	
						652	**55.3065**	**6.14**	
45	3/16/18	Sturm	utarak Divide, Lin	68.1950	-152.5217	188	63.159	16.07	
46	3/16/18	Sturm	utarak Divide, Lin	68.1950	-152.5217	271	69.85	7.735	
						459	**66.5045**	**11.9025**	
47	3/18/18	Sturm	Creek Divide, Li	68.5683	-150.2350	102	71.035	11.15	
48	3/18/18	Sturm	Creek Divide, Li	68.5683	-150.2350	216	82.522	17.36	
						318	**76.7785**	**14.255**	
49	3/6/18	Pedersen	aktuvuk Pass, Nc	68.5526	-150.6051	753	46.42	28.66	Low-shub tundra
50	3/6/18	Pedersen	Nanushuk River	68.4801	-151.2765	598	40.17	30.44	Tussock tundra
51	3/9/18	Pedersen	/est of Ernie Pas	68.1053	-151.0138	557	26.49	29.90	Low-shub tundra
52	3/9/18	Pedersen	tuvuk River NPS	68.1488	-151.6389	504	19.02	12.47	Low-shub tundra
53	3/10/18	Pedersen	Anaktuvuk Pass	68.1168	-151.3449	527	25.05	21.03	Low-shub tundra/Tussock tundra
54	3/10/18	Pedersen	aktuvuk Pass, Sc	68.2822	-151.4873	494	13.58	7.05	Tussock tundra
55	3/11/18	Pedersen	lik River and Ana	68.5208	-150.8942	544	57.00	10.04	Low-shub tundra
56	3/12/18	Pedersen	: of Itkillik River V	68.5776	-150.1452	427	94.70	13.30	Low-shub tundra/Tussock tundra
57	3/14/18	Pedersen	tkillik River, Nortl	68.5919	-149.8277	525	41.31	17.89	Low-shub tundra/Tussock tundra
58	3/15/18	Pedersen	tkillik River, Sout	68.3501	-150.0011	442	10.46	4.91	Low-shub tundra/Tussock tundra
59	3/18/18	Pedersen	irktok River Valle	68.2563	-148.8718	746	38.82	16.06	Low-shub tundra/Tussock tundra
60	3/18/18	Pedersen	iirktok River Valle	68.5067	-149.0421	526	24.45	10.37	Low-shub tundra
61	3/19/18	Pedersen	r Valley at moun	68.3724	-148.9459	576	19.23	12.41	Low-shub tundra/Tussock tundra
62	3/20/18	Pedersen	on River Valley, S	68.7126	-148.6031	412	68.67	19.89	Low-shub tundra/Tussock tundra
63	3/21/18	Pedersen	on River Valley, I	68.6329	-148.2913	374	87.93	9.57	Low-shub tundra/Tussock tundra
64	3/22/18	Pedersen	ishak River, Sou	69.0345	-147.8586	299	88.44	16.77	Low-shub tundra
65	3/22/18	Pedersen	'ishak River, Nor	69.0326	-147.8049	372	66.00	24.28	Tussock tundra
66	3/23/18	Pedersen	Lupine River	69.0617	-148.7950	462	59.51	8.34	Low-shub tundra
67	3/23/18	Pedersen	‹ River, South of	69.0753	-148.5257	535	89.60	10.08	Low-shub tundra/Tussock tundra
68	3/24/18	Pedersen	k River, North of	69.2106	-148.8103	441	69.48	11.02	Low-shub tundra/Tussock tundra
69	3/24/18	Pedersen	ktok River, Pump	69.3632	-149.2688	485	58.33	8.37	Tussock tundra
70	3/25/18	Pedersen	Toolik River	69.0416	-149.4281	419	81.14	10.88	Low-shub tundra/Tussock tundra
71	3/25/18	Pedersen	/est of Toolik Riv	69.4491	-148.5743	495	49.80	8.54	Low-shub tundra/Tussock tundra
72	3/25/18	Pedersen	pper Kuparuk Riv	68.6503	-149.3640	453	47.37	11.49	Low-shub tundra/Tussock tundra
73	3/26/18	Pedersen	Creek, Sveta Stu	68.5848	-149.3056	476	66.89	11.84	Low-shub tundra
74	3/28/18	Pedersen	Wiseman	67.4233	-150.1110	10	75.67	2.64	Spruce forest
75	4/1/18	Pedersen	Chandalar Lake	67.4926	-148.5077	308	56.41	10.61	Spruce forest
76	4/1/18	Pedersen	alar Shelf, north	67.9616	-149.0650	456	59.73	12.97	Low-shub tundra
77	4/2/18	Pedersen	Fork of Chandala	67.7891	-148.4330	390	62.35	7.31	Spruce forest
78	4/2/18	Pedersen	rth of East Butto	67.3758	-149.0574	606	88.53	16.87	Spruce forest
79	4/3/18	Pedersen	Crow Nest Creek	68.0423	-146.0044	551	65.43	6.04	Spruce forest
80	4/3/18	Pedersen	Lake, Junjik Rive	68.3701	-146.4519	886	50.96	8.23	Low-shub tundra
81	4/4/18	Pedersen	Chandalar River	67.2273	-148.4153	620	63.80	14.38	Spruce forest
82	4/4/18	Pedersen	Bob Johnson Lak	67.4793	-149.3278	1062	59.66	13.01	Mixed spruce forest/low-shrub tundra
83	4/5/18	Pedersen	st of Slope Moun	68.7078	-149.0046	1137	60.01	35.09	Low-shub tundra
						18468	**55.21**	**14.08**	
84	5/3/18	Sturm	‹ Point just S. De	70.4947	-149.8812	**605**	**33.3**	**10.99**	low tussock tundra
85	5/2/18	Sturm	Barrow near ARM	71.322	-156.62	**1239**	**45.18**	**11.6**	low tussock tundra

Shifting focus to the data collected in the area shown in Figure 2, we can explore the character of the snow cover in greater detail. For these stations two orthogonal depth transects were measured, along with SWE and stratigraphy. The data are summarized in Table II. As these stations were near or in the Brooks Range, the mean depth value (67.3 cm) is higher than in Figure 5, but well-matched by the mean snow pit depth (67.9 cm, *n*=13), suggesting in general snow pit locations were representative of the larger surrounding neutral areas where we chose to measure.

Table II: Near-Brooks Range Station Snow Statistics

Station	Latitude (N)	Longitude (W)	Snow Pit Depth (cm)	Core Ave. Depth (cm)	Pit Bulk Density (g/cm3)	Core Bulk Density (g/cm3)	Mean-All Probe Depths (cm)	Std. Dev. - All Probe Depths (cm)	***n*** (All Probe Depths)
Nanashuk Divide	68° 33.6'	150° 33.0'	54	54.6	0.280	0.239	52.6	10.6	320
Nanashuk Bottom	68° 33.1'	150° 36.4'	36						
Barchan A	68° 28.8'	151° 17.0'	89		0.437				
Barchan B	68° 28.8'	151° 17.0'	78		0.405				
Ernie Pass	68° 06.0'	150° 59.8'	102	84.5	0.377	0.308	74.8	27.5	241
Greylime Headwall	68° 07.8'	150° 48.8'	139	125.7	0.297	0.297	110.7	39.9	98
Ekokpuk	68° 01.3'	152° 21.1'	50	62.2	0.258	0.253	62.8	13.2	676
Amiloyak Lake A	68° 06.1'	152° 54.0'	45	54.2	0.265	0.224	47.2	9.3	393
Amiloyak Lake B	68° 06.1'	152° 54.0'	55		0.296				
Agiak	67° 57.6'	153° 02.2'	53	40.4	0.255	0.232	56.0	17.5	484
July Creek Divide	67° 52.1'	153° 32.4'	69	49.7	0.214	0.176	55.5	7.3	532
Kollutarak Divide	68° 11.7'	152° 31.3'	53	61.5	0.269	0.222	67.1	12.3	459
May Creek Divide	68° 34.1'	150° 14.1'	60	62.6	0.296	0.240	78.8	16.5	318
AVERAGES			**67.9**	**66.2**	**0.304**	**0.243**	**67.3**	**17.1**	**3521**

Using the two orthogonal lines measured at each station, we have examined how much the local depth statistics might have been altered due to a minor shift in sampling location (Fig. 7). The results suggest a consistency in mean depth and standard deviation between the two adjacent lines of ±10 cm (for mean) and ±5 cm (std. deviation) respectively. These results would indicate that care needs to be taken when assuming that a depth value from a single spot location is used to represent the depth over a larger area. Small shifts in instrument location could readily introduce differences in depth of greater than ±10 cm, and that is when making several hundred depth measurements. When considering the potential error in the mean when a ***single*** measurement is made (like from a sonic sounder), a simple statistical experiment with real data (Fig. 8) suggest the size of the error: at the Ekokpuk Creek station, the mean depth was 62.8 cm (*n*=676). The distribution curve for these data is shown in Figure 8, and is basically normally distributed. Hence there would be a 32% probability of a single spot measurement being at least ±13 cm different than the mean, and a 5% chance that it will differ by ±26 cm (±41%). This is a point we return to later when examining the data reported by existing autonomous networks as compared to the field results.

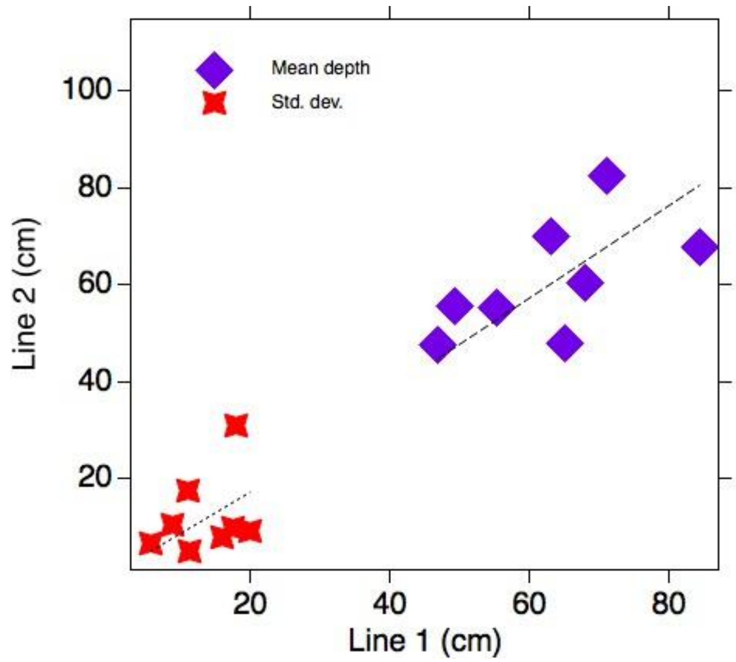

Figure 7:Depth statistics from the two orthogonal lines measured at each near-Brooks Range station. The black dashed lines are the 1:1 lines for the data. The results suggest that differences of ±10 cm in the mean (or more) occurred, but that the high or low bias varied in a random way from one station to another.

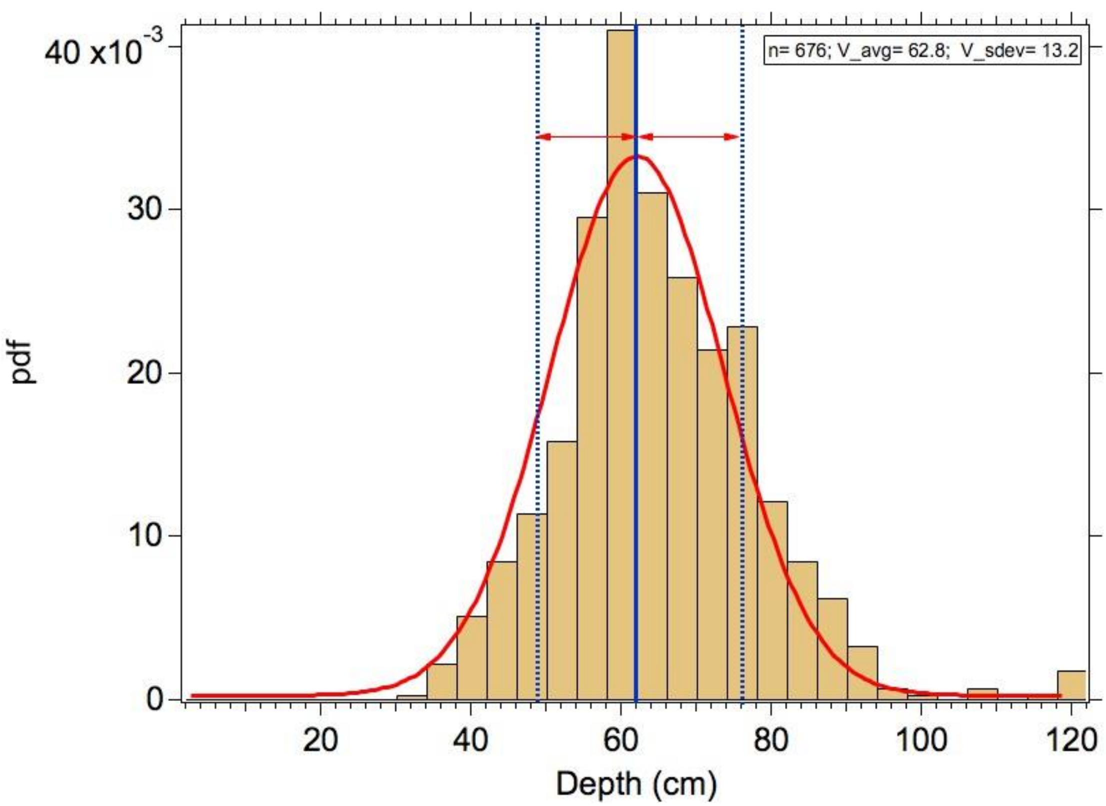

Figure 8: Depth distribution for measurements taken at Ekokpuk Creek along several probe lines, showing that spot depths differing from the mean by ±13 cm would have occurred 32% of the time.

The mean bulk snow density from these stations was 0.304 g/cm^3. This value is not surprising as the mean bulk seasonal snow density across all of North America typically falls around 0.3 g/cm^3 The stations for which we have density valies lie mostly in the foothills and Brooks Range where the snow is less wind-affected and less dense than closer to the coast. The mean bulk density for snow closer to the coast, based on data taken in 2014-2015 is often closer to 0.35 g/cm3 (Fig. 9).

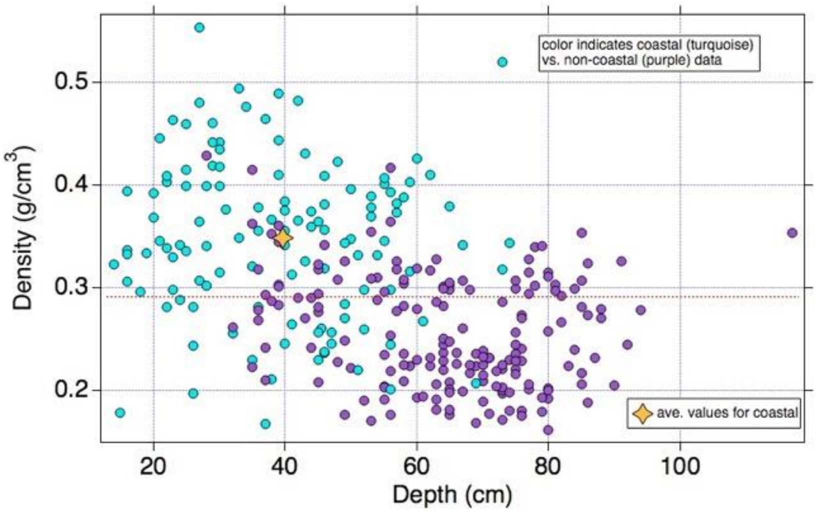

Figure 9: Bulk snow pack densities from Federal coring data collected in 2014 and 2015 in the Arctic National Wildlife Refuge by the lead author, showing the difference in bulk densities nearer the coast than in the foothills and the Brooks Range. The red dotted line is the mean for all data.

Density values in 2018 determined by coring were consistently lower than those computed from snow pit layer densities, most probably due to the high percentage of fragile depth hoar comprising the lower part of the snow pack. Even though we rejected all core samples that did not have a plug, it is likely that the downward travel of the core barrel through the snow forced some of the loose depth hoar away from the barrel, reducing the sampled mass. We have corrected this core low bias (see below) based on the pit densities, which we believe to be more accurate. For the 10 snow pits for which a direct comparison could be made, we found this regression equation did an adequate job of correction:

*Corrected Core Density = 1.142 * Measured Core Density* (r^2=0.95) [1].

Essentially, the core-based densities were 14% low. Using the corrected SWE values from coring, and the measured depth values, we then fit the resulting data with a quadratic function:

*SWE (cm) = 6.8 + 0.002451*Depth (cm)^2* [2],

which captures the fact that the deeper snow (>80 cm) was denser than the shallower snow, primarily because the deeper snow contained more drift layers. The slope of the fitted curve for depth values less than 80 cm is about 0.26 (essentially a bulk density in g/cm^3), but for the deeper snow (> 80 cm), the slope is 0.47 g/cm^3, a value consistent with the higher density of drift snow we have measured elsewhere.

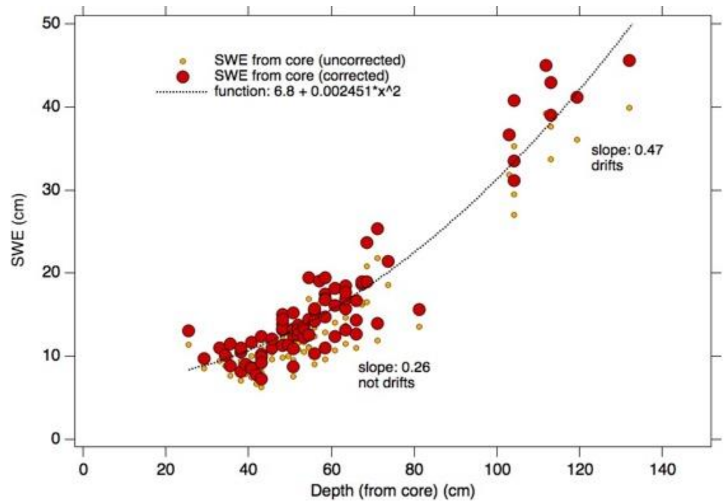

Figure 10:Corrected core-based SWE values plotted against the measured depth at each core. The quadratic fit (black dotted line) is given in Equation [2] and captures the fact that deeper snow is generally comprised of more drifted snow, hence denser. The slope of the fitted line gives (roughly) the bulk density for that depth value and can be used to convert depths to SWEs.

We can use the results from Tables I and II and Figure 10 to make a general statement about the SWE of 2018. The mean depth of the full data ensemble was 53.5 cm, which when multiplied by the measured core bulk density (0.304 g/cm^3) suggests an ensemble mean SWE of 16.3 cm. Allowing for the fact that much of the full area is not in the Brooks Range or foothills, we might compute a slightly higher value using the coastal density of (53.5 cm X 0.350 g/cm^3 (Fig. 9)), suggesting a mean SWE value closer to 18.7 cm. For the Brooks Range and foothills, this value is slightly greater due to the deeper snow: (0.304 g/cm^3 X 67.3 cm), or 20.5 cm. Perhaps the most representative way to compute the region-wide value is to convolve the log normal depth probability distribution in Figure 6 with the power function for converting depth to SWE (Figure 10). This produces an average region-wide SWE value of ***17 cm***. From this, we can then estimate how much snow (in the form of water) was residing across the study area by late-April 2018. Multiplying the SWE with the regions area we find about ***42 km^3*** of water in the form of snow. Since the sampling did not include drifts, which are deeper and denser 50% higher, or over ***60 km^3*.**

The stratigraphic results from the snow pits are summarized in Table III and shown in Figures 11a and 11b. On average, the pack had 9 distinct, recognizable layers, each averaging about 7.8 cm in thickness, and on average the SWE (cm) was 22.2 cm for the pit, a value just slightly higher than that determined by coring (with correction). The measurements show that on average the pack was comprised of 66% depth hoar, 26% wind slab, with new/recent snow and some fine-grained soft layers making up the small remainder. The highest slab fraction, 65%, was measured at Ernie Pass, where two thick slab layers, already somewhat metamorphosed into compact and indurated depth hoar, comprised 54 cm of the total 102 cm depth of the pit. We suspect that even a slight relocation of the pit would have reduced this slab fraction considerably due to the pinching and swelling common in such wind slabs. We find it notable that in an area generally considered windy, such soft, friable depth hoar layers, not wind slabs, were the predominant snow texture. This is a fact that has important bearing on the survival strategies of many of the local sub- and supra-nivean wildlife, and suggests the value of obtaining textural values for the Arctic snow pack.

While we lack data from nearer the coast, prior work indicates we could expect the slab percentage to rise and the depth hoar percentage to fall with increasing distance north. In that prior work, the depth hoar fraction ranged from 34 to 44%. This difference should not be weighted too heavily: the classification of the layers in a pit into depth hoar and wind slab is complicated by a common feature of the snow in this region, which is wind slabs that have metamorphosed into depth hoar. Depending on the degree of metamorphism, these can be classified by observers as slabs, or as depth hoar, creating some ambiguity in the fractional distribution of snow layer types. These slabs are often compact, under a hand hardness test may be finger- or pencil-hard, and may register 0.4 g/cm^3 or higher in density, yet the grains in the layer may be more than a centimeter in length and show strong and skeletal faceting typical of depth hoar. From an traverse done in 1994 where many snow pits were measured for texture, we have constructed a south-to-north cross section of snow texture (Brooks Range to Arctic Coast) that shows the increasing amount of wind slab with distance north, as well as the issue with indurated depth hoar (Fig. 12).

Table III: Stratigraphic Results

Station:	Total thickness (cm)	Number of Layers	Ave. layer thickness (cm)	Bulk Density (g/cm3)	SWE (cm)	Wet/Icy Fraction	New/Recent Fraction	Other Fraction	Hoar Fraction	Slab Fraction
Nanashuk Divide	54	9	6.0	0.280	15.1	0.01	0.00	0.08	0.70	0.20
BarchanA	89	7	9.9	0.437	38.9	0.00	0.00	0.00	0.44	0.56
BarchanB	78	7	8.7	0.405	31.6	0.00	0.00	0.00	0.56	0.44
Ernie Pass	102	12	11.3	0.377	38.4	0.02	0.00	0.04	0.29	0.65
Greylime Headwall	139	9	15.4	0.297	41.3	0.00	0.12	0.00	0.74	0.14
Ekokpuk Creek	50	11	5.6	0.258	12.9	0.00	0.02	0.00	0.92	0.06
Amiloyak Lake A	45	10	5.0	0.265	11.9	0.00	0.02	0.07	0.62	0.29
Amiloyak Lake B	55	10	5.5	0.296	16.3	0.00	0.02	0.07	0.51	0.40
Agiak Creek	53	9	5.9	0.255	13.5	0.00	0.06	0.04	0.87	0.04
July Creek Divide	69	10	7.7	0.214	14.7	0.00	0.07	0.10	0.70	0.13
Kollutarak Divide	53	10	5.9	0.269	14.3	0.00	0.08	0.08	0.79	0.06
May Creek Divide	60	9	6.7	0.296	17.8	0.00	0.05	0.00	0.78	0.17
	70.6	**9.4**	**7.8**	**0.304**	**22.2**	**0.003**	**0.036**	**0.039**	**0.661**	**0.261**

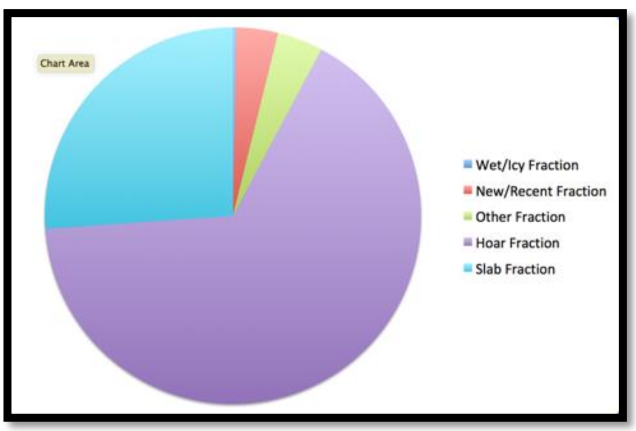

Figure 11a: Snow layer textures based on pit measurements.

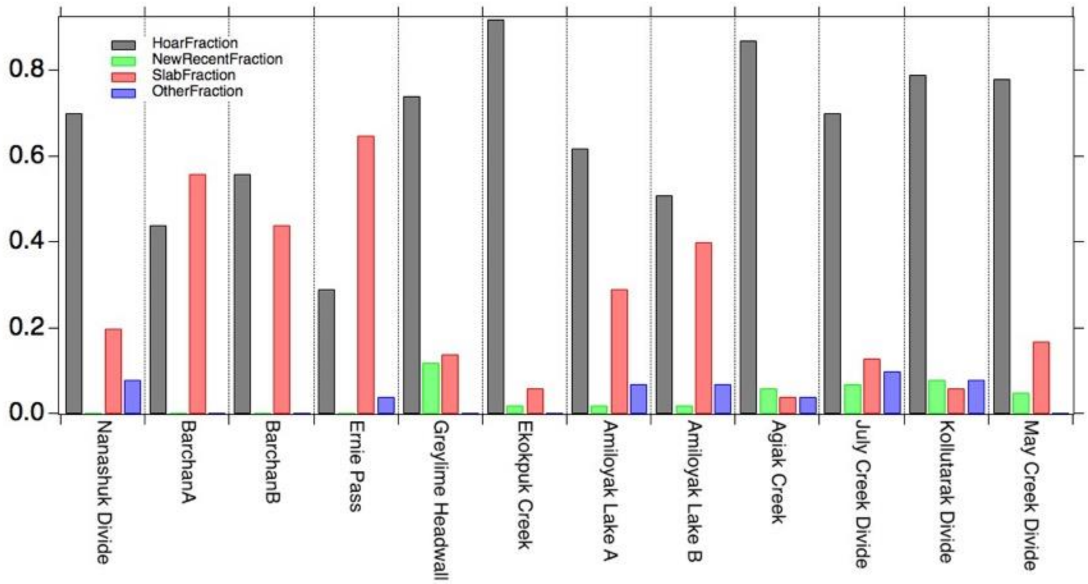

Figure 11b: Layer textures by snow pit and station.

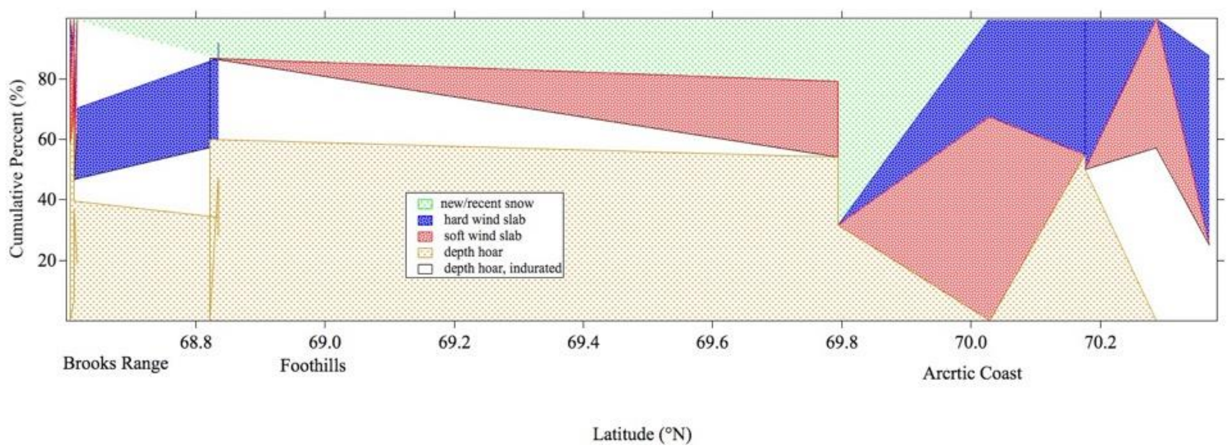

Figure 12: Wind slab and depth hoar percentages from the Brooks Range to the Arctic Coast, April 1994.

While this lower-than-expected fraction of wind slab layers in and near the Brooks Range is a bit surprising, it is useful to examine the stratigraphy of one of the hard dunes encountered during the 2018 field work to understand something of the nature of these slabs. A notable feature of the snow landscape in 2018 was the presence of large barchans. These were more common than in previous years. Barchans are crescent-shaped dunes that form during wind transport of snow and are transitional between snow waves and circular or elongated dunes that are more common. We encountered fields of these barchans during our March traverse, and again in April near Toolik Lake. These barchans were quite hard (walking over them left no footprints: Fig. 13) and fairly extensive. At one location, we sectioned a barchan (Figs. 13 and 14) to see if the hard layers extended to depth. The cross section shows that an exceptionally dense slab (0.59 g/cm^3) capped the dune (note that the upper theoretical limit on seasonal snow density in the absence of melting is about 0.56 g/cm^3), but below, the layers were not as dense or as hard. Even in this exceptionally hard drift, two soft depth hoar partings were present, and the basal unit, which had at one time been a hard slab, had metamorphosed into a hoar layer that near its base was quite friable and weak. We infer from the cross section that during the 2017-2018 winter there had been unusually strong transport winds and abundant snow to supply the wind-blown flux, a fact confirmed (see below) from drift surveys.

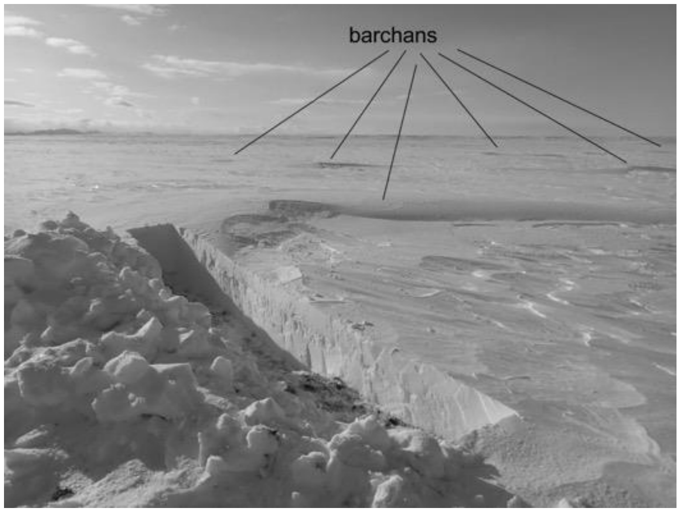

Figure 13:The barchan dune field and the barchan we sectioned using a saw and axe. The trench is 1 m deep.

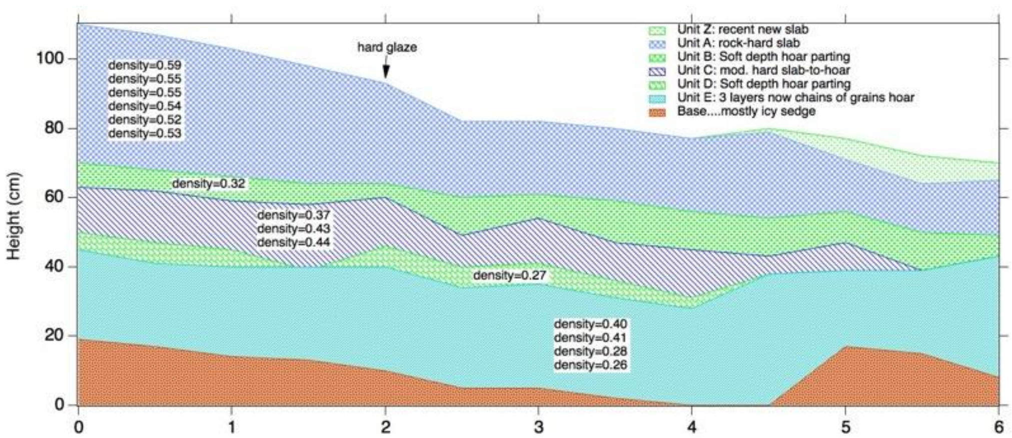

Figure 14: Cross-section of the dune shown in Figure 13, showing the density of the layers. Horizontal axis is meters; vertical axis is cm with 3X exaggeration.

The second to final results from the field work concern wind direction. Two factors govern the nature of this regional snow cover: 1) ***time***, in that long periods of residence under strong temperature gradients create depth hoar from virtually any snow that has been deposited, and 2) ***wind***, which a) determines where there will be scour or drift, and b) creates dense hard layers that resist depth hoar development, hence has some control on the ***time*** effect. Given that there are few locations where the wind direction is actually measured, modeling snow numerically (with wind speed and direction as an input) can be problematic. Fortunately, wind direction (if not wind strength) can be deduced directly from features in the snow: dunes and sastrugi, cornices, and crag and tail features to name a few (Fig. 15).

Figure 15:These crag-and-tail features that formed around shrub clusters are at the headwaters of Easter Creek and indicate the wind was from left to right.

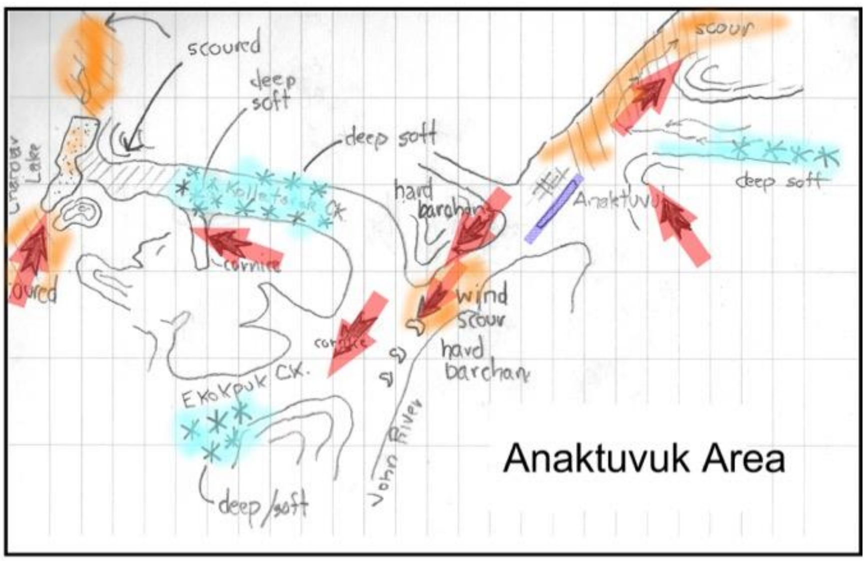

Figure 16: A field sketch (modified) of drift and scour features near Anaktuvuk Pass made in March 2018. Red arrows indicate wind directions deduced from drift features. Blue areas were deep, low-density snow; tan areas scour zones. Note that wind directions are complex and unlikely to be correctly indicate by measurements made at the local airport (purple strip).

In Figure 16, one of our field sketch maps of observed features and implied wind directions is shown. A first impression following this mapping suggests the following points that have modeling implications:

1. Katabatic flow dominates in the northeast-southwest trending valleys, but vectors indicate transport occurs in both directions. The dividing line between the flow directions is uncertain. We have similar effects in the Arctic National Wildlife Refuge, particular in the Marsh Creek area where scour on the north (downslope) side of the Sadlerochit Mountains is pervasive.
2. East-west trending valleys had deeper, softer snow…and more shrub vegetation…but there were still local areas of wind scour in these valleys in unexpected locations.

3. Considerable "turning" of the wind could be deduced from the observations, with wind directions being altered by flow over ridges, across slopes and down valleys. This turning was clearly indicated by cornice size and direction.
4. While we could map wind directions from snow features, new snow obscured some of these features, and we could not ascertain when snow from earlier in the winter had drifted in a different direction than the snow later in the winter.

Lastly, we present a sample of the SfM snow depth mapping we conducted during the 2018 field work. This photogrammetric technique for snow mapping requires that a snow-free digital elevation map (DEM) be produced (one time only) then subtracted from any subsequent DEM mapping done in winter to produce a snow depth map. One area we measured (April 23-26, 2018) is the area shown in Figure 17, a swath running from Camden Bay a south to Marsh Creek across the 1002 area of the Arctic National Wildlife Refuge, with the Sadlerochit Mountains just south of the swath.

Figure 17: Location map for the aerial mapping of snow depth shown in Figure 18. The mapped area is shown in red.

.

The mapping results (Fig. 18) show an extremely heterogeneous snow cover with depths ranging from near-zero to more than 5-m in the drifts lining the cutbanks of Marsh Creek. This is an area where seismic exploration is proposed for 2018-2019. The katabatic scouring from the Sadlerochit Mountains is clearly evident in the southern part of the map area (red colors), where considerable areas of the tundra have < 25 cm (9.8") of snow cover, despite the fact that 2017/2018 was a year of record deep snow. Such a snow cover poses significant issues for human over-snow travel and work.

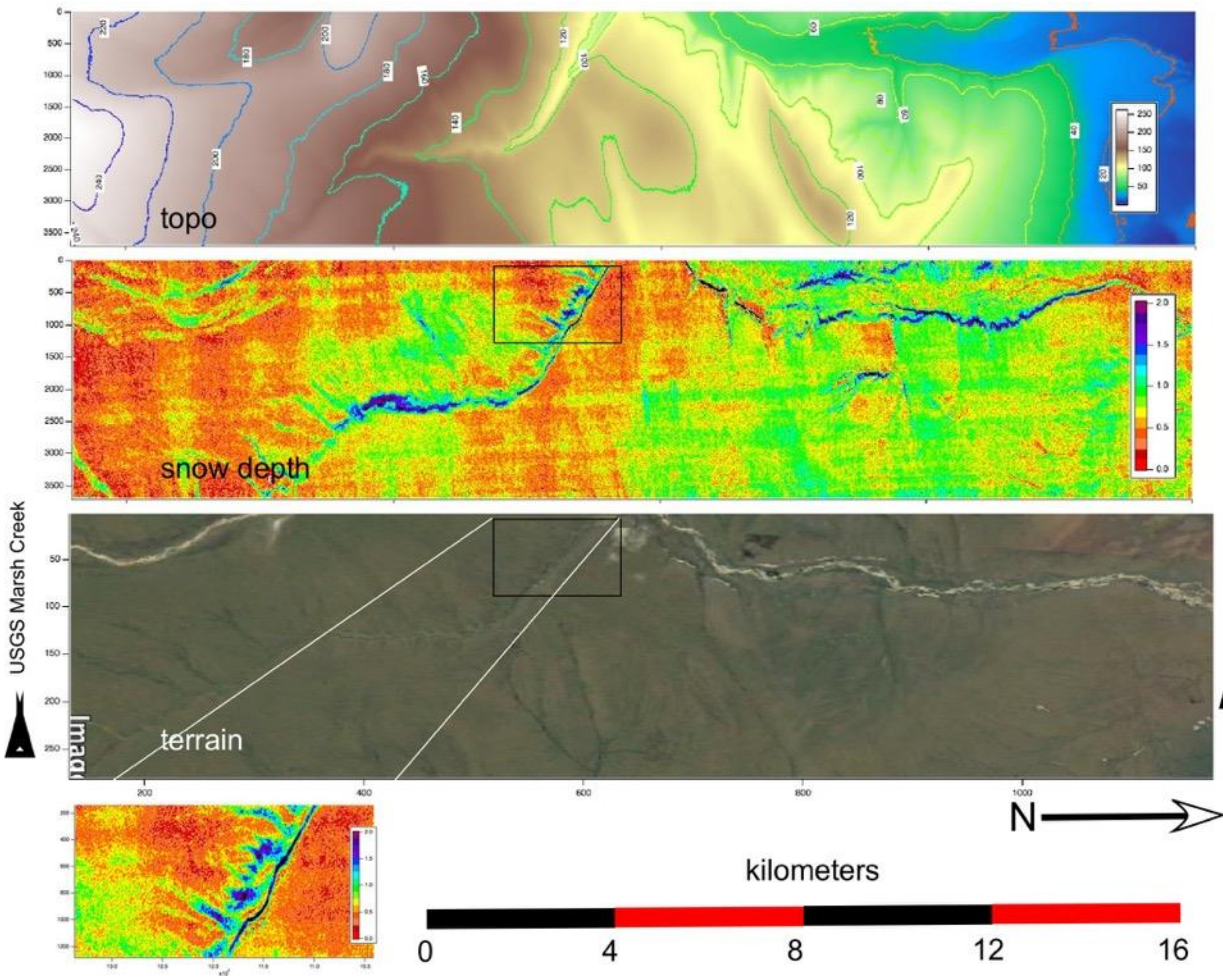

Figure 18: April 2018 structure from motion snow depth map for the swath shown in Figure 17 crossing the 1002 area of the Arctic National Wildlife Refuge. The top panel is the topography; the middle panel the snow depth (accurate to ±10 cm), and the lower panel the same area in a Landsat image. The snow depth ranges from near-zero (red) to more than 5 m deep (black) and varies over short (<20 m) distances. Note the extensive scour zones on the south (left side) end of the swath, as well as scour zones downwind (NE) of the large drifts lining Marsh Creek. North is to the right.

Comparison of Field and Autonomous Data: The results of the traverse provide a rare in-depth view of the snow cover of the region, but for only a single moment in time. We would ask whether we would be able to derive a similar perspective from the autonomous weather stations operating in the region. To answer this question, we polled the snow depth data from the RAWS stations lying within several hundred kilometers of the traverse region for the month of March (Fig. 19). Table IV lists these stations. Of the 13 stations examined, four (4) were not equipped with a sonic snow depth sensor nor precipitation gauge and had to be discarded. Three (3) additional stations had sonic sensors, but these were not working, leaving six (6) stations for which snow depth data was obtained. On top of the daily depth values from these stations we have plotted the values obtained during our March traverse (each plotted on the dates the measurements were made). We note that during this month there was little additional snowfall, and relatively little wind, so drift transport was limited, hence little reason to expect temporal variation in RAWS depths.

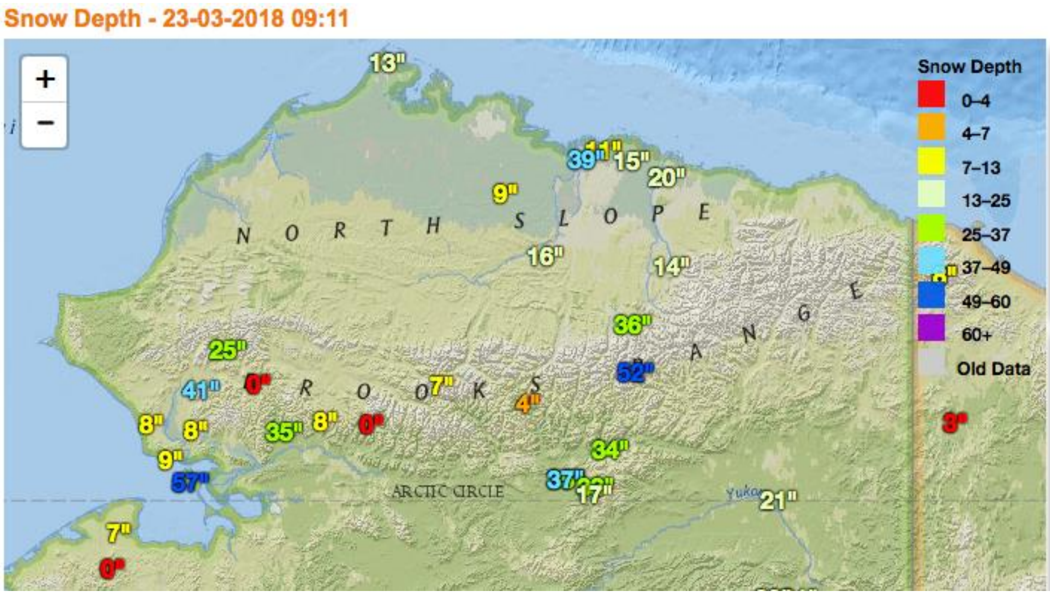

Figure 19: Screen shot from the NOAA-National Weather Service website showing the limited amount of snow data available for the Brooks Range (source: https://www.weather.gov/aprfc/Snow_Depth).

Table IV: RAWS Stations Used in Comparison with Field Data

Station	NESS ID	Latitude	Longitude	Status
Killik Pass,	3961C1E8	67° 58' 13"	154° 55' 27"	data available
Umiat	326B17F6	69° 22' 12"	152° 08' 10"	data available
Pamichtuk Lake	3961E704	67° 46' 19"	152° 11' 42"	data available
Imelyak	3961316C	67° 32' 46"	157° 04' 09"	data available
Inigok	32522240	70° 00' 13"	153° 05' 01"	data available
Kugururok	396203F8	68° 19' 00"	161° 29' 31"	data available
Chimney Lake	3961F472	67° 45' 21"	150° 29' 36"	not working
Ram Creek	3961D29E	67° 41' 07"	154° 28' 23"	not working
Howard Pass	39617266	68° 09' 22"	156° 53' 45"	not working
Noatak	FA601340	68° 04' 15"	158° 42' 15"	no sonic depth sounder
Norutak Lake	3246B586	66° 50' 00"	154° 20' 00"	no sonic depth sounder
Helmut Mountain	126006F2	67° 44' 29"	144° 07' 21"	no sonic depth sounder
Kanuti	1260A60A	66° 05' 36"	152° 10' 12"	no sonic depth sounder

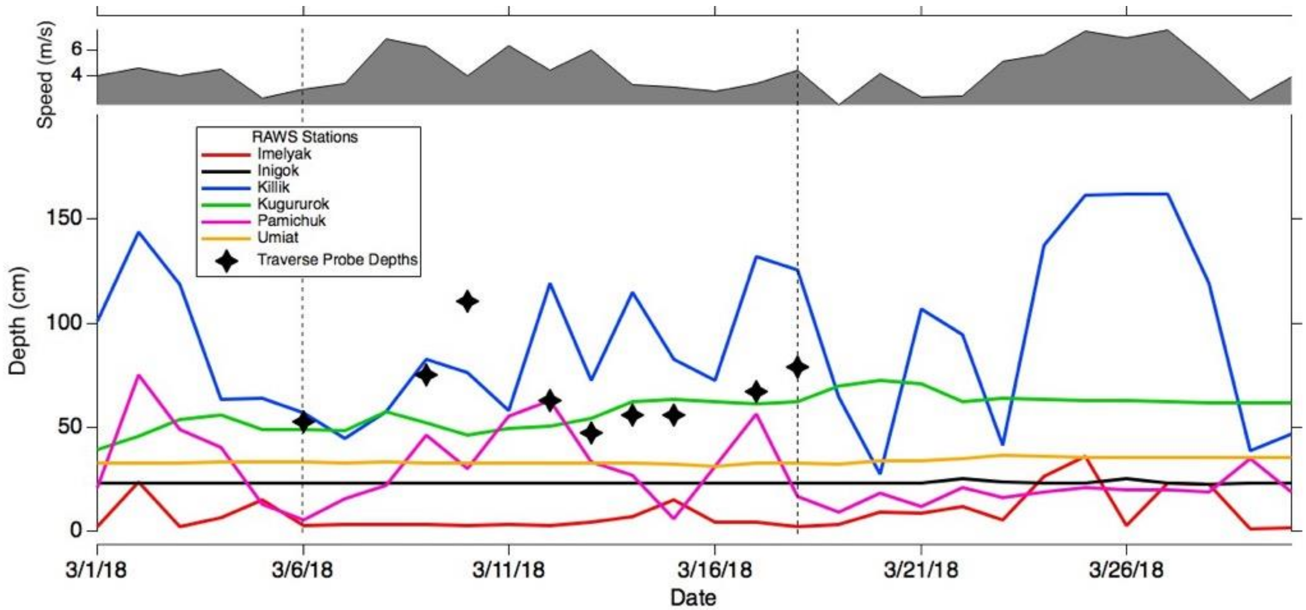

Figure 20: RAWS snow depth data (colored lines) compared to depths measured at traverse stations (black symbols). The variation in the traverse data is spatial in nature, while the variation in each RAWS station depth is temporal. Considering that little snow fell during March, and the wind was generally less than 6 m/s (transport speed), the large variations in depth for the Pamichuk and Killik RAWS stations are likely to be spurious.

The results (Fig. 20) show large (±50 cm) near-daily variations in depth at the RAWS Killik station and almost as large (±30 cm) variations at the Pamichuk station, fluctuations that are unlikely to be real. The Umiat and Inigok stations lie well north of the mountains out on the Arctic coastal plain, and show, as we would expect, shallower snow. The extremely steady values at Inigok (black line) are suspicious. Imelyak records almost no snow, probably not a real result for a station in the Brooks Range. The Kugururok station provides the best match to most of the traverse data, and appears quite believable. The issue, however, would be whether a user would know to use the Kugururok data while discarding the other stations. It is unclear how that data decision might be reached without ancillary data.

The NRCS runs three totalizing precipitation gauges spanning the east edge of the traverse area: Atigun Pass, Imnaviat Creek, and Sagwon, all sites we have visited and at times monitored in collaboration with the NRCS. At Atigun Pass, the March and April snow depth values (134 cm) were the same because there was little snowfall during the month. This value compares favorably with our measured value from the Greylime Headwall traverse station, which is at about the same elevation, and in the same physiographic position as the Atigun NRCS station. The Imnavait NRCS station increased from 89 to 96 cm depth over the month of March, suggesting a mid-March value of just over 90 cm, a value that is a bit high compared to our local station data for comparable elevations and physiography. The NRCS Sagwon site was registering 35 cm of snow depth throughout March. Like the more northerly RAWS stations, this value is lower than any of the traverse depth data, but the lower value is consistent with its position well north of the Brooks Range. SWE was not available for these stations at the time of this writing.

Our conclusion from this brief comparison is that while the autonomous data available for the traverse region could provide a "picture" of the regional snow pack, data reliability causes difficult problems in achieving that result. In some ways, using the NRCS data alone currently would provide a better snapshot of the snow depth in the area than using all the data because they appear to be more reliable. This is not a surprise. The RAWS sites were not designed to capture snow depth data; they are typically on a local hilltop (Fig. 21), a good place to measure the local wind, but a poor place to measure snow because it is often scoured away by the wind. It is also unclear if when the RAWS sites were installed, much care was taken to ensure that the rock piles holding the tower did not create drifts or scour under the sonic sounder. Finally, it is unclear why large fluctuations in depth values were observed when the snow was unchanging, but we suspect this is due to some electronic issues.

Figure 21: The Howard Pass RAWS station (courtesy DRI website). Snow depth sensor is on the arm projecting left. The gold-topped bucket is an unshielded precipitation gauge.

This issue of using data from autonomous stations has direct management implications across the entire region, both for human activity and wildlife management. Absent some human "check", it is clear to us that relying on the autonomous instruments could lead to erroneous decisions. For example, opening the tundra for seismic exploration based on a spot measurement from a sonic sounder that has produced a false positive (or negative) could lead to an opening when in fact management stipulations have not been met.

The Winter of 2017-2018: A Climatological Context

The deeper snowpack observed at Imnavait Creek in April 2018 as compared to April 2017 is consistent with higher precipitation measured at the Imnavait Creek Snotel site (Fig. 22), and supports the idea that the 2017-2018 winter had higher than usual precipitation. As assessed over the period 1 October through 30 April, total precipitation over the 2016/2017 snow year was 2.9 inches vs. 4.5 inches over the 2017/2018 snow year. Note that because of gauge under-catch, these measured values (both winters) are likely low by a factor of around 2.3X. The most notable event during the 2016/2017 snow season was a 0.4 inch event recorded for January 3, 2017 (Fig. 22 left) associated with a low pressure system in the Beaufort Sea. In contrast, during the 2017/2018 snow season there were more precipitation events (Fig. 22 right) with a large number of events early in the season. Of note was an event of 0.3 inches precipitation on October 14 (Fig. 23). The synoptic pattern giving rise to these events is not especially clear, but a deep low pressure over eastern Siberia seems to be involved; note the upward (negative) omega at 600 hPa over the Imnavait Creek area, which is a measure of the upward motion of air masses, consistent with cooling, condensation and precipitation. This was followed by an event of 0.2 inches on October 17-18 of 2018, associated with a low over the eastern Beaufort Sea (on the 17th) and (apparently) formation of a new low to the west on the 18th. These, and several other events, produced deeper snow cover over much of northern Alaska; the results highlight that just one or two large events can produce significant increases in snow depth in this generally thin-snow region.

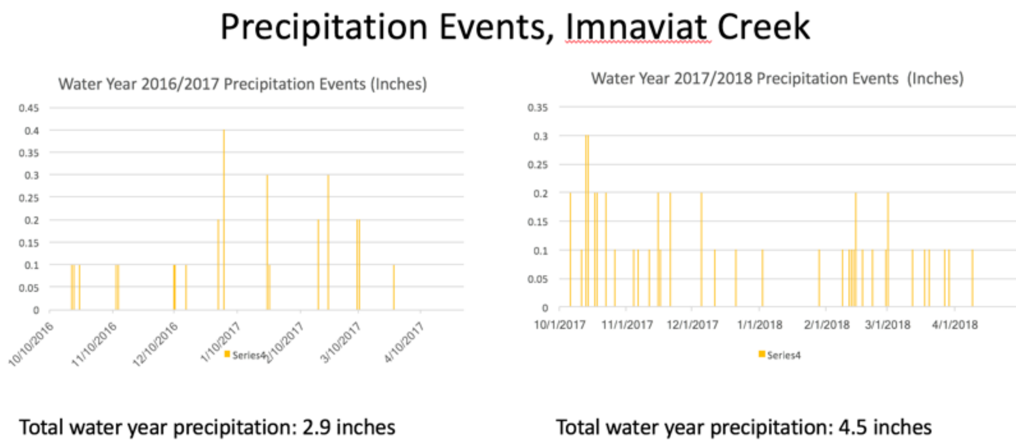

Figure 22: The measured precipitation at the Snotel site at Imnavait is low by a factor of about 2.3. This is based on comparisons with measured SWE at Imnavait in April, and assumes that all precipitation that falls from 1 October through 30 April accumulates as snow, Using this factor, the total precipitation for the 2016/2017 and 2017/2018 snow season, respectively, is likely to have been closer to 6.7 inches and 10.3 inches (17.0 and 26.2 cm) respectively. Based on average recorded snow depths of 62.7 and 76.2 cm, this yields mean densities of 270 and 340 kg m-3, respectively.

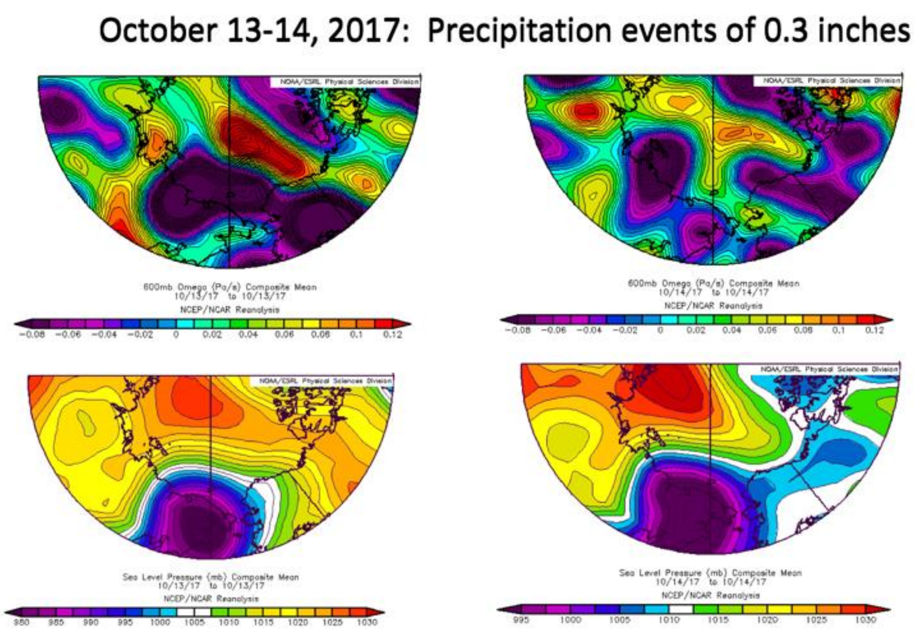

Figure 23: The first of two back-to-back large precipitation events early in the 2017/2018 winter.

Despite a limited ability to place the snow cover of 2017/2018 in a climatological context, there are other indicators besides the precipitation record that indicate it was an exceptionally heavy snow year, and a year when wind transport was near-record high. One measure that suggests this is a comparison of the April 2018 snow depth value for the 1-by-1 km test grid at Imnavait Creek near Toolik Lake (Fig. 24). We have been making measurements in this area since 1983. The 2018 value is the highest on record (though there are some gaps in the record). Near the test grid we have also been monitoring a large drift that forms in the lee of a cutbank (called the S-2 drift). It was the second largest on record over a 28-year period (during which we managed to survey the drift 15 times). In Barrow, the drift in the lee of the Cakeater Road snow fence was also all-time record largest (Fig. 25), and the snow depth at the local NWS weather station on April 1 was 10 cm higher than the 30-year norms (35.6 cm vs. 25.9) (http://climate.gi.alaska.edu/stations/barrow).

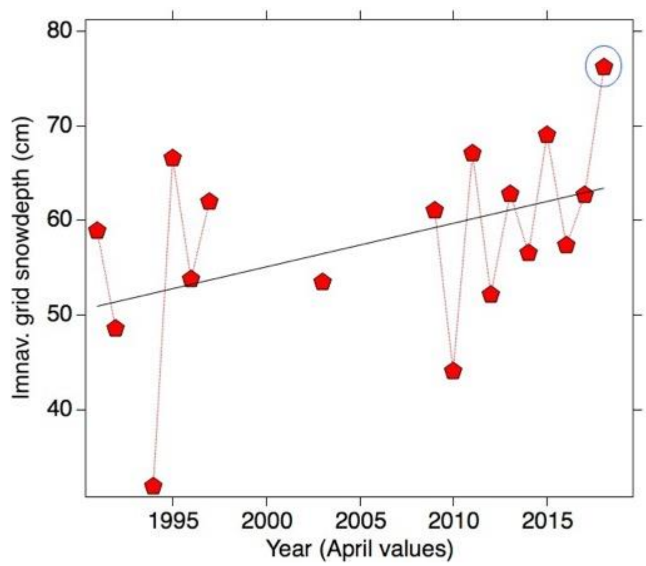

Figure 24: The mean snow depth from measurements made in the 1-by-1 km grid at Imnavait Creek. Not only is the 2018 value the highest in the record, but also there appears to be a trend for increasing snow depth.

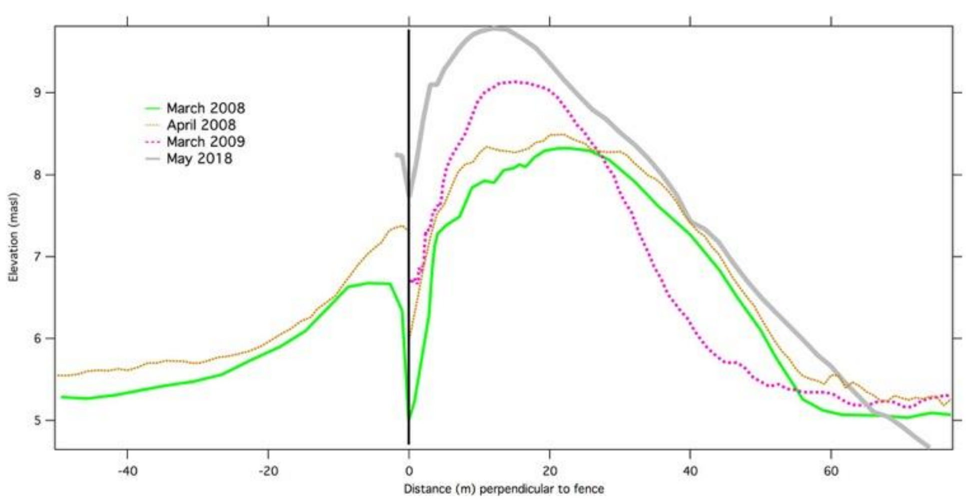

Figure 25: Cross section profiles from the Cakeater snow drift near Barrow showing the very large drift (record) from 2018.

Isotope Results and Storm Tracks:

The isotope results indicate that:

- isotope ratios on the south side of the Brooks Range were generally depleted compared to those on north side (Fig. 26a and Table V).
- there was greater variability in isotopic values late in the winter (top layers) as opposed to the earlier in the winter (bottom layers) (Fig. 26b and Table V).
- there was evidence that snow in late winter on the south side of the Brooks Range was the most depleted in $\delta^{18}O$.

These results suggest that the winter moisture sources differ between the north and south sides of the Brooks Range in early winter, but this difference fades as the winter progresses (Table V). Specifically, *d-excess* values from early winter (5.8 on the north, 7.7 on the south) indicate different moisture sources N. and S. of the range, but these values then converge later in winter. Our interpretation is that early winter the moisture source on the N. side of the Brooks Range is in part the largely open ice-free (and humid) Chukchi Sea. This produces the lower *d-excess* values. The S. side of the Brooks Range receives early winter snow sourced from the interior of the eastern Yukon Territory (Canada), which is relatively cold and arid. As winter progresses, the cold interior Yukon moisture sources continue on the S side of the Brooks Range hence the *d-excess* values vary little throughout winter (Table 5). However, there is ***a moisture source switch*** on the N side of the Brooks Range that leads to changes in isotopic values there: that snow pack it is more oceanic in the early winter and then switches to moisture from the Yukon region later in winter.

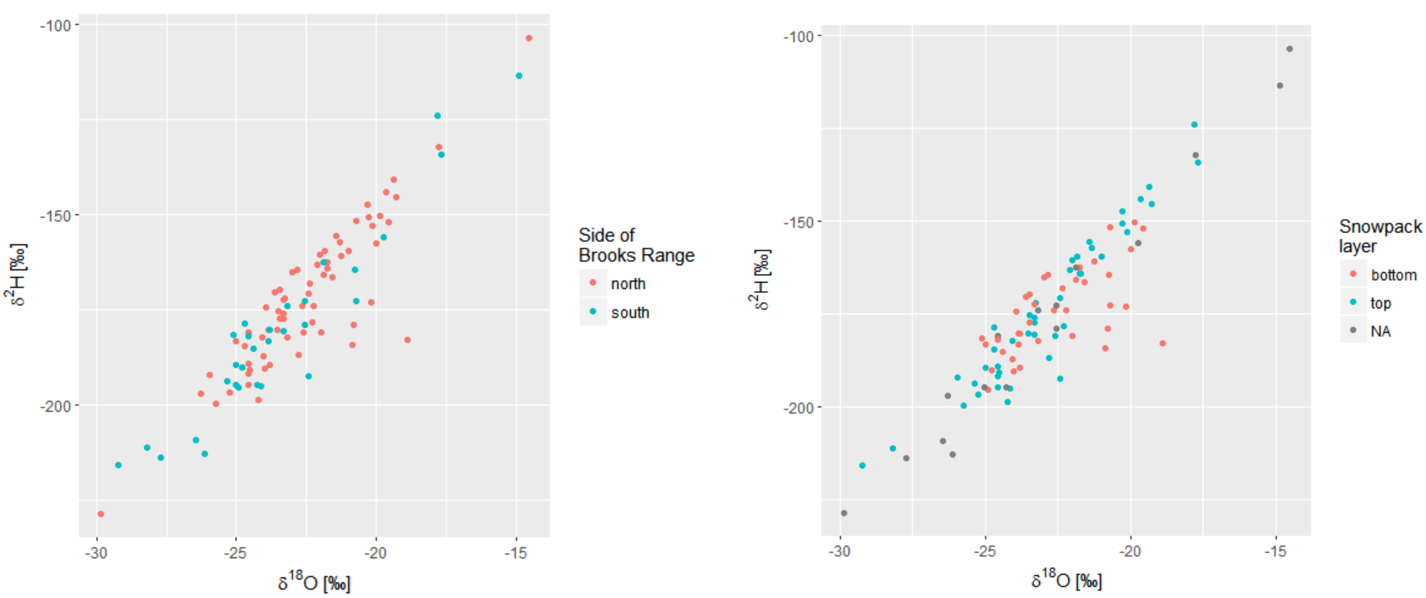

Figures 26a (left): Co-isotope plot with north (red) and south (blue) sides of the Brooks Range in different colors. Fig. 26b (right): Co-isotope plot with samples from the early winter (bottom) and the late winter (top) snowfall. 'NA' are samples from layers in between top and bottom.

Table V: Averages for $\delta^{18}O$, δ^2H, and *d-excess* for all samples north and south of the Brooks Range, with ± indicated by the standard error of the mean (SE), and then the values separated by north vs. south and the bottom (early winter) and the top (late winter) of the snow pits.

	North	South	North: bottom layer	South: bottom layer	North: top layer	South: top layer
n	68	30	29	9	34	10
Average $\delta^{18}O$ ±SE [‰]	-22.5±0.3	-23.5±0.6	-22.2±0.3	-23.7±0.6	-22.6±0.3	-23.8±1.2
Average δ^2H ±SE [‰]	-171.8±2.3	-181.0±4.5	-171.9±2.1	-181.6±3.0	-172.1±3.0	-181.3±9.5
Average *d-excess* ±SE [‰]	7.9±1.1	7.1±1.4	5.8±2.2	7.7±2.5	9.1±1	9±3.2

Conclusions: The Brooks Range and North Slope winter of 2017-2018 produced a record snowfall, and (possibly) record large drifts. This occurred due to just a few additional, and slightly stronger, precipitation events. Whether the drifts were larger because there was more snow, more wind, or both, is uncertain. We might have been able to reach this conclusion about the snow conditions from the various autonomous instrument that operate in the area, but because they produced conflicting (and erroneous) results, working from those data alone would have resulted in a high degree of uncertainty at best, or perhaps complete wrong conclusions. Moreover, those autonomous instruments and measurements are unable to tell us about the density, texture, and other aspects of the snow that directly affect human activities (like over-snow travel) and wildlife (like caribou cratering). Currently, that appears to be possible only by putting humans on the ground, and argues for human monitoring in concert with the other instruments.

Despite the record snowfall, large areas of the domain exhibited patchy and often thin snow (Fig. 18) late in the winter of 2017/208 due to the action of the wind. These thin areas exist adjacent to deep drifts in the lee of cutbanks, and the two extremes can be thought of as conjugates since they are linked by wind transport processes. Such extremes in depth pose serious issues for proposed seismic activities related to oil and gas development.

Finally, some land management agencies, for a number of reasons, find the permitting of snowmobile enabled ground measurement programs problematic, but the necessity for measurements at many locations makes similar aerial-based campaigns extremely dangerous. Our view is that a) we need humans on the ground to measure snow if we are to really understand the winter environment of northern Alaska and how it is changing, b) that the safest way to do this is via snowmobile traverses, and c) that such activities are necessary to meet the monitoring and inventorying requirements for these public lands. Such human monitoring is particularly important at this time because massive changes in the sea ice conditions across the Arctic Ocean appear (Figs. 24a and 24b) to have already altered the winter environment of the region.

Acknowledgements
Carrie Voyuvich, Kelly Elder, Glen E. Liston, Kaj Lynöe, Luke Metherell, Dirk Nickisch, and Miranda Weiss assisted in the field work. Rick Thoman helped us to understand katabatic scouring. As always, we had excellent support from the staff at Toolik Field Station. We also had help from many people in Anaktuvuk Pass, including Charlie Sollie Hugo. We thank the ARM site operators for data from Barrow and Oliktok Point, and continue to owe a large debt all of the people who try to keep the weather stations in this remote region of the Arctic operating in such tough conditions.

The Geonor precipitation gauge at Oliktok Point in April 2018, completely drifted over by the winter's heavy snow…but still sending out (erroneous) autonomous data.